Syntheses, Structures, and Porous/Luminescent Properties of Silver 3-Alkyl-1,2,4-Triazolate Frameworks with Rare 3-Connected Topologies

ARTICLE *in* CRYSTAL GROWTH & DESIGN · JANUARY 2011

Impact Factor: 4.89 · DOI: 10.1021/cg101435b

7 AUTHORS, INCLUDING:

Xiao-Lin Qi
University of Aveiro
16 PUBLICATIONS **325** CITATIONS
SEE PROFILE

Ai-Xin Zhu
Yunnan Normal University
20 PUBLICATIONS **384** CITATIONS
SEE PROFILE

Jing Wang
The Second People's Hospital of Jingzhou,C…
419 PUBLICATIONS **6,220** CITATIONS
SEE PROFILE

Xiao-Ming Chen
Sun Yat-Sen University
421 PUBLICATIONS **22,444** CITATIONS
SEE PROFILE

DOI: 10.1021/cg101435b

CRYSTAL GROWTH & DESIGN Article

2011, Vol. 11
796–802

Syntheses, Structures, and Porous/Luminescent Properties of Silver 3-Alkyl-1,2,4-Triazolate Frameworks with Rare 3-Connected Topologies

Jie-Peng Zhang,* Xiao-Lin Qi, Zhi-Juan Liu, Ai-Xin Zhu, Yan Chen, Jing Wang, and Xiao-Ming Chen

MOE Key Laboratory of Bioinorganic and Synthetic Chemistry, State Key Laboratory of Optoelectronic Materials and Technologies, School of Chemistry and Chemical Engineering, Sun Yat-Sen University, Guangzhou 510275, China

Received October 28, 2010; Revised Manuscript Received December 25, 2010

ABSTRACT: Self-assembly of silver(I) ion with 3-alkyl-1,2,4-triazoles in different solvents yielded four new metal azolate frameworks (MAFs), namely, [Ag(mtz)] (**1**, Hmtz = 3-methyl-1,2,4-triazole), [Ag(etz)] (**2**, Hetz = 3-ethyl-1,2,4-triazole), $[Ag_4(etz)_4]\cdot H_2O$ ($\mathbf{3}\cdot H_2O$), and $[Ag_4(ptz)_4]$ (**4**, Hptz = 3-propyl-1,2,4-triazole). Single-crystal X-ray diffraction revealed that Ag(I) ions and triazolates in these MAFs are all three-coordinated to give rare 3-connected framework topologies. Although **1** and **2** possess the same uniform (10,3)-d (**utp**) topology, variation of the alkyl groups renders substantially different coordination structures. On the other hand, $\mathbf{3}\cdot H_2O$ and **4**, also bearing different alkyl substituents, are isomorphours, and can be simplified as the same uninodal sqc5603 topology (point and vertex symbols are 8^2.10 and 8.8_2.12, respectively). Due to the relatively short alkyl length, the coordination framework of $\mathbf{3}\cdot H_2O$ contains one-dimensional narrow channels. According to thermogravimetry and single-crystal X-ray diffraction, $\mathbf{3}\cdot H_2O$ can be dehydrated without framework collapse. Although guest-free **3** does not adsorb N_2 at 77 K, $\mathbf{3}\cdot H_2O$ can undergo guest exchange, and **3** can adsorb solvent vapor, to give CH_2Cl_2- and CH_3CN-included crystals. Comparing the single-crystal structures of $\mathbf{3}\cdot H_2O$, **3**, $\mathbf{3}\cdot CH_2Cl_2$, and $\mathbf{3}\cdot CH_3CN$ reveals the framework flexibility of **3**. These materials also show interesting structure- and guest-dependent photoluminescent properties.

Introduction

Coordination polymers (CPs) have attracted much attention due to their intriguing structures and interesting properties.[1] While remarkable achievements have been attained, controlling the framework structure and understanding the structure−property relationship remain fundamental challenges due to the complexity of self-assembly and the resultant structures. Network topology has been demonstrated as a powerful tool for the analysis and design of complicated structures.[2] Although simple and highly symmetric topologies are the most accessible synthetic targets, many of such topologies remain rarely reported or unprecedented.

Metal azolate frameworks (MAFs), being composed of transition metal ions and deprotonated five-member heterocycles, are a unique subset of CPs.[3] In addition to the strong coordination ability toward transition metal ions, azolate ligands also combine the negative charge of carboxylates and predictable coordination modes of pyridines. The fixed coordination geometries of azolato rings further reduce the structural diversity of MAFs. Therefore, the chemical compositions and network connectivities of MAFs can be reasonably predicted. The structures of binary MAFs are a function of the charges and coordination geometries of the involved metal ions and azolates. Imidazolates and pyrazolates both act as 2-connected linkers, which can be combined with univalent coinage metal ions to give closed (i.e., ring) or extended chains. The metal ions linked by imidazolate and pyrazolate have separations of about 6 and 3−4 Å, and angles of about 140 and 70°, respectively, making a big difference on the porosity of the resultant frameworks. Accordingly, imidazolate can link tetrahedral metal ions to form porous zeolitic structures,[3b,4] but pyrazolates usually form oligomeric clusters or dense structures.[3a,5] Nevertheless, polypyrazolates, being similar to polycarboxylates, are very effective bridging ligands for the generation of porosity.[6,7] In contrast with the 2-connected diazolate linkers, 1,2,4-triazolates usually behave as 3-connected nodes because the three nitrogen donors are involved in coordination.[8] Moreover, the Y-shaped coordination geometry of 1,2,4-triazolate is significantly different with a regular triangle. Consequently, uncommon 3-connected networks may be straightforwardly constructed by univalent coinage metal 1,2,4-triazolates, in which both the metal and triazolate act as the 3-connected nodes. Although the node-to-node separations are the shortest ones (ca. 3.1 and 3.4 Å for cuprous and silver triazolates, respectively) among all types of CPs, coinage metal triazolate frameworks are relatively 'porous' due to the low topology density of 3-connected nets. However, due to interpenetration or blockage effect of bulky substituent groups,[9] only a few coinage metal triazolate frameworks have been demonstrated as porous materials.[10]

Compared to other types of ligands, the noncoordinated substituent groups attached on the short azolate ligands are usually located close to each other and then have significant interactions within the coordination networks, which play crucial roles in directing the superstructures of MAFs.[4b,11] While ligand design for common ligands is usually meant to control the linking geometry and/or separation length of multiple coordination groups, modifying the noncoordinated substituent groups represents the main strategy for the crystal engineering of MAFs. For example, cuprous 1,2,4-triazolates usually consist of rigid planar dimeric secondary building units, which can be regarded as square-planar nodes. The

*To whom correspondence should be addressed. E-mail: zhangjp7@mail.sysu.edu.cn.

 Published on Web 01/18/2011

Table 1. Crystallographic Data and Refinement Parameters

	1	2	3·H_2O	3	3·CH_2Cl_2	3·CH_3CN	4
formula	$C_3H_4AgN_3$	$C_4H_6AgN_3$	$C_{16}H_{26}Ag_4N_{12}O$	$C_{16}H_{24}Ag_4N_{12}$	$C_{17}H_{26}Ag_4Cl_2N_{12}$	$C_{18}H_{27}Ag_4N_{13}$	$C_{10}H_{16}Ag_2N_6$
FW	189.96	203.99	833.97	815.95	900.88	857.01	436.03
T/K	293(2)	143(2)	293(2)	293(2)	293(2)	293(2)	103(2)
space group	$Pna2_1$	$Pna2_1$	$C2/c$	$C2/c$	$C2/c$	$P2_1/c$	$C2/c$
a/Å	11.1121(13)	7.1495(4)	13.1876(10)	13.0358(14)	12.9651(8)	11.9318(6)	13.6250(15)
b/Å	10.9483(12)	8.1326(4)	21.3132(15)	21.135(2)	21.4537(14)	21.3132(15)	21.1810(16)
c/Å	3.8187(5)	9.5939(5)	11.7034(8)	11.7194(13)	11.7302(7)	11.6563(6)	11.9294(11)
β/deg	90	90	122.828(1)	122.184(1)	122.632(1)	113.844(1)	108.73(3)
V/Å^3	464.58(10)	557.83(5)	2764.1(3)	2732.7(5)	2747.7(3)	2720.6(2)	2850.5(5)
Z	4	4	4	4	4	4	8
D_c/g cm^{-3}	2.716	2.429	2.004	1.983	2.178	2.092	2.032
μ/mm^{-1}	4.181	3.491	2.823	2.851	3.034	2.870	2.740
$R_1{}^a$ ($I > 2\sigma$)	0.0235	0.0119	0.0284	0.0520	0.0266	0.0284	0.0369
$wR_2{}^b$ (all data)	0.0636	0.0302	0.0726	0.1313	0.0701	0.0650	0.0872
GOF	1.079	1.037	1.042	1.048	1.008	1.024	1.046
Flack parameter	0.05(9)	−0.04(3)					

$^a R_1 = \sum||F_o| - |F_c||/\sum|F_o|$. $^b wR_2 = [\sum w(F_o^2 - F_c^2)^2/\sum w(F_o^2)^2]^{1/2}$.

steric hindrance between the substituent groups of the triazolate ligands can control the dihedral angles between the square-planar nodes, and then lead to different extended topology. Changing the substituent groups from hydrogen atoms to methyl, ethyl, and propyl groups give two-dimensional (2D) **sql-a**, three-dimensional (3D) **lvt-a**, and 3D **nbo-a** networks.[9] So far, reported binary metal 1,2,4-triazolates are all based on symmetric/disubstituted ligands.[12] Only a few ternary MAFs have been constructed by the unsymmetric 3-amino-1,2,4-triazolate[8a−c] and 3-methyl-1,2,4-triazolate.[8d] As an extension of our continuous investigations on MAFs, we studied the self-assembly of Ag^+ ions with a series of unsymmetric 3-alkyl-1,2,4-triazolates (methyl, ethyl, and propyl). Four new MAFs with novel 3-connected topologies and/or interesting porous and luminescent properties have been successfully constructed and characterized.

Experimental Section

Materials and Physical Measurements. Commercially available reagents were used as received without further purification. 3-Alkyl-1,2,4-triazoles were synthesized by a reported method.[13] Thermal gravimetric (TG) analysis was performed under N_2 using a NETZSCH TG 209 system. Powder X-ray diffraction (PXRD) patterns were measured using a Bruker D8 Advance diffractometer (Cu−Kα). Gas sorption isotherms were measured by Belsorp MAX volumetric adsorption equipment. Photoluminescence profiles were recorded at room temperature by an FSP920 combined time-resolved and steady-state spectrometer (Edinburgh Instruments) equipped with a 450 W Xe lamp.

Synthesis of [Ag(mtz)] (1, Hmtz = 3-methyl-1,2,4-triazole). An aqueous ammonia (25%, 10 mL) solution of $AgNO_3$ (0.0850 g, 0.5 mmol) was mixed with a methanol solution of Hmtz (0.0415 g, 0.5 mmol) to give a clear solution, which was allowed to stand in the dark for 7−10 days. Colorless needle-like crystals were filtered, washed with methanol, and dried in air (0.0645 g, yield 68%). Elemental analysis (%) for $AgC_3H_4N_3$ (calc: C, 18.97, H, 2.12; N, 22. 12; found: C, 18.98; H, 2.24; N, 22.06).

[Ag(etz)] (2, etz = Hetz = 3-ethyl-1,2,4-triazole). The reaction was carried out using the same method used for **1** (0.0765 g, yield 75%), except that Hmtz was replaced by Hetz (0.0485 g, 0.5 mmol). Elemental Analysis (%) for $AgC_4H_6N_3$ (calc: C, 23.55, H, 2.96; N, 20.60; found: C, 23.79; H, 2.96; N, 20.85).

[Ag_4(etz)$_4$]·H_2O (3·H_2O). The reaction was carried out in the same method as for **2** (0.0782 g, yield 75%), except that methanol was replaced by ethanol (15 mL). $Ag_4C_{16}H_{26}N_{12}O$ (calc: C, 23.04, H, 3.14; N, 20.16; found: C, 23.08; H, 3.04; N, 20.01).

[Ag_4(ptz)$_4$] (4, Hptz = 3-propyl-1,2,4-triazole). The reaction was carried out using the same method used for **1** (0.0817 g, yield 75%), except that Hmtz was replaced by Hptz (0.0555 g, 0.5 mmol). Elemental analysis (%) for $AgC_5H_8N_3$ (calc: C, 27.55, H, 3.70; N, 19.27; found: C, 27.65; H, 3.54; N, 19.37).

X-ray Crystallography. Diffraction intensities were collected on a Bruker Apex CCD area-detector diffractometer (Mo−Kα). The structures were solved by direct method, and all non-hydrogen atoms were refined anisotropically by least-squares on F^2 using the SHELXTL program.[14] Hydrogen atoms on organic ligands were generated geometrically. Solvent exchange for 3·H_2O was carried out by immersing 3·H_2O single crystals in corresponding solvent at room temperature. Solvent adsorption for **3** was carried out by exposing single crystals of **3** in corresponding solvent vapor in a sealed bottle at room temperature. Simulated PXRD patterns were generated by Mercury 2.3. Crystallographic data and refinement details are summarized in Table 1.

Results and Discussion

Syntheses and Structures. It has been shown that an aqueous ammonia solution of metal salt is beneficial for the crystal growth of MAFs.[3b] In this study, four structures have been discovered by reactions of the aqueous ammonia solution of $AgNO_3$ with 3-alkyl-1,2,4-triazoles in different solvents (H_2O, MeOH, EtOH, and acetone). For Hmtz and Hptz, single phases of [Ag(mtz)] (**1**) and [Ag_4(ptz)$_4$] (**4**), respectively, were isolated in all tested solvents. In contrast, MeOH and EtOH solutions of Hetz gave rise to a dense structure [Ag(etz)] (**2**) and a porous structure [Ag_4(etz)$_4$]·H_2O (3·H_2O), respectively. It is interesting that EtOH induces the formation of a porous structure but it is not included in the crystal lattice, implying that EtOH may serve as an additive or structural directing agent for the formation of 3·H_2O. Phase purities of the as-synthesized samples were confirmed by PXRD patterns (Figures S1−4, Supporting Information).

Compound **1** crystallizes in a polar space group $Pna2_1$, containing one Ag^+ ion and one deprotonated mtz^- ligand in the asymmetric unit (Figure S5). The Ag^+ ion is trigonally coordinated by three nitrogen donors from three μ_3-mtz^- ligands (Ag−N 2.224(4)−2.245(4) Å, N−Ag−N 115.34(15)−123.18(16)°). As 1,2,4-triazolates combine the coordination modes of pyrazolates and imidazolates, dividing the complicated structures by smaller fragments is usually helpful. Considering mtz^- as a pyrazolate-type linker first, Ag^+ is connected by Ag−N^1 and Ag−N^2 bonds into a 2_1 helix (Figure 1a), which further interconnects with four neighbors (as pseudo-4_1 helices) with opposite chirality, via Ag−N^4 and N^4−Ag bonds, to form the 3D structure. This connection manner is similar to the 8^2.10-a (**lig**) topology observed

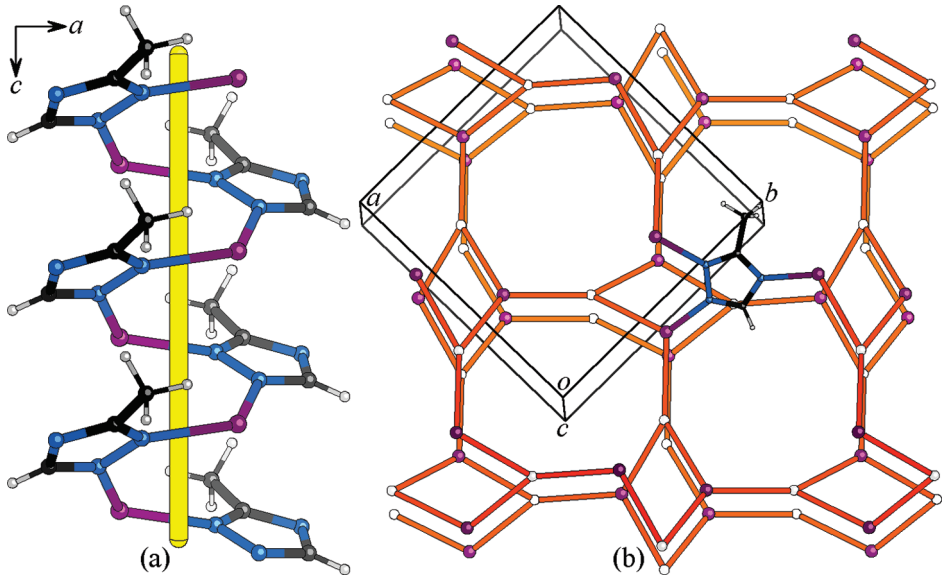

Figure 1. Perspective views of (a) a helical chain fragment linked by the pyrazolate moiety of mtz^- and (b) the **utp** network structure of **1** (mtz^- ligands except one are simplified as white spheres).

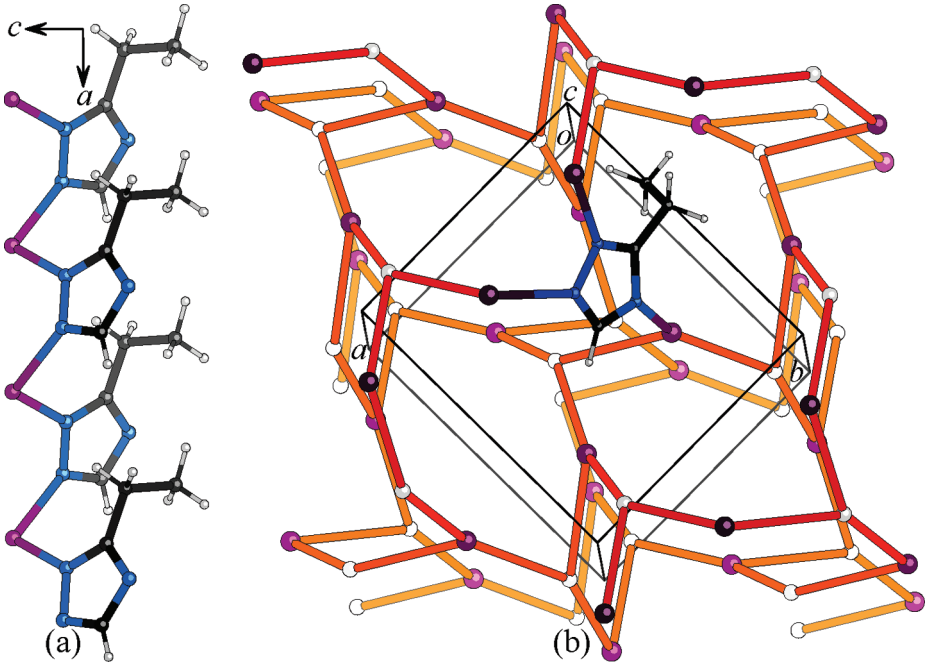

Figure 2. Perspective views of (a) a zigzag chain fragment linked by the pyrazolate moiety of etz^- and (b) the **utp** network structure of **2** (etz^- ligands except one are simplified as white spheres).

in β-[Cu(dmtz)].[15] However, the topology of **1**, regarding both Ag^+ and mtz^- as 3-connected nodes, is a rarely observed uniform 3-connected (10,3)-d (**utp**) net (Figure 1b).[16] The two closely related nets arise from the different offsets of adjacent 4_1 helices, which produce eight-membered rings for **lig** and $8_1/8_7$ helices for **utp**. The well-known uniform 3-connected (10,3)-a (**srs**) net is constructed by linking homochiral 4_1 helices.[2a] Due to the short node-to-node separation, significant framework distortion, and blockage of methyl groups, **1** is nonporous. Supposing an edge length of 3.4 Å, the unit-cell volume of the most expanded configuration of **utp** should be 745 $Å^3$, which is much larger than that for **1** (V = 465 $Å^3$), confirming the significant framework distortion.

Compound **2** also crystallizes in the space group $Pna2_1$, with one three-coordinated Ag^+ ion and one μ_3-etz^- ligand in the asymmetric unit (Figure S6). However, the coordination geometry of Ag^+ should be described as T-shaped (Ag−N 2.144(5), 2.159(6), 2.431(6) Å; N−Ag−N 154.4(2), 108.1(2), 97.4(2)°). Ag^+ is connected by the pyrazolate moiety of etz^- into a zigzag chain (Figure 2a), being contrast to the fashion for **1**. Surprisingly, the MAF topology of **2** is also **utp** (Figure 2b), in which the pseudo-4_1 helices are linked by the imidazolate moiety of etz^- (N^2 and N^4). **2** is also nonporous for the same reason as for **1**. Nevertheless, to accommodate the longer ethyl groups, the silver triazolate scaffold in **2** (V = 558 $Å^3$) is less contracted than for **1** (V = 465 $Å^3$).

Compound $\mathbf{3}\cdot H_2O$ crystallizes in the space group $C2/c$, with two Ag^+ ions, two etz^- ligands, and half of a water molecule in the asymmetric unit (Figure S7). All Ag^+ ions are

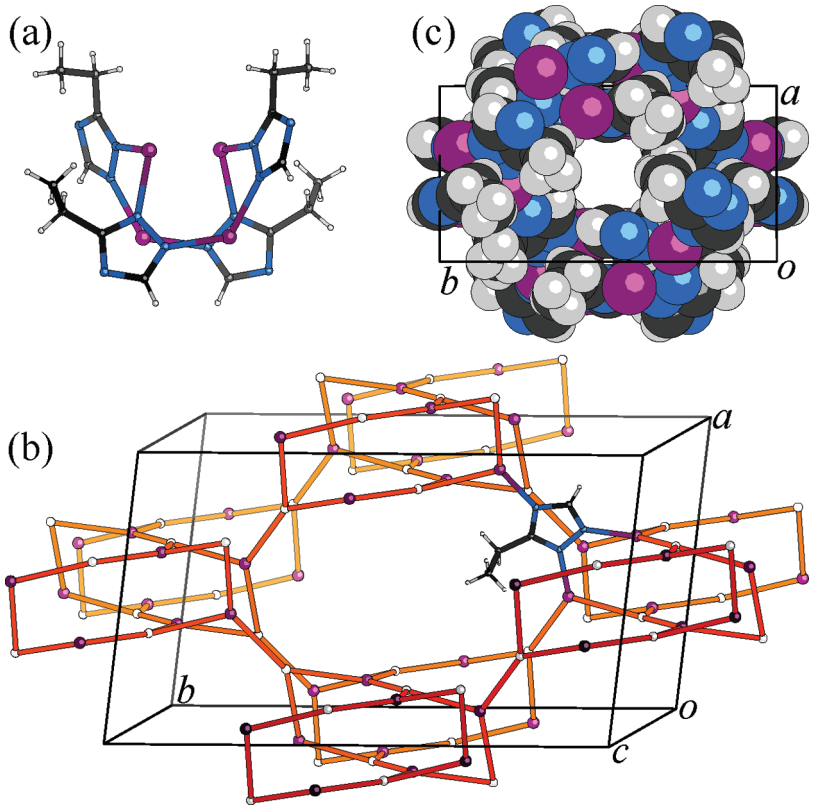

Figure 3. Perspective views of (a) a cyclic $Ag_4(etz)_4$ fragment linked by the pyrazolate moiety of etz^-, (b) the sqc5603 network structure (etz^- ligands except one are simplified as white spheres), and (c) the one-dimensional (1D) channel (disordered guest molecules are omitted) running along the *c*-axis of $\mathbf{3}\cdot H_2O$.

Table 2. Characteristics of Some Representative Topologies[18,19]

net	coordination	space group	Wyckoff	volume[a] [Å^3]	node density [Å^{-3}]
bcu	8	$Im\bar{3}m$	2a	1.5396	1.2990
pcu	6	$Pm\text{-}\bar{3}m$	1a	1.0000	1.0000
nbo	4	$Im\bar{3}m$	6b	8.0000	0.7500
lvt	4	$I4_1/amd$	8c	12.3200	0.6494
qtz	4	$P6_222$	3c	4.0001	0.7500
dia	4	$Fd\text{-}\bar{3}m$	8a	12.3168	0.6495
ANA	4	$Ia\text{-}\bar{3}m$	48g	84.1486	0.5704
SOD	4	$Im\bar{3}m$	12d	22.6268	0.5303
RHO	4	$Im\bar{3}m$	48i	112.5880	0.4263
LTA	4	$Pm\text{-}\bar{3}m$	24k	56.1247	0.4276
srs	3	$I4_132$	8a	22.6268	0.3536
utp	3	*Pnna*	8e	18.9662	0.4218
sqc5603	3	$I4_1/amd$	32i	83.5946	0.3828
lig	3	$I4_1/amd$	16f	45.2544	0.3536
nbo-a	3	$Im\bar{3}m$	24g	112.5670	0.2132
lvt-a	3	$I4_1/amd$	32i	168.6400	0.1898

[a] The cell volume of topology with edge length 1 Å.

coordinated in distorted trigonal-planar coordination geometries (Ag−N 2.165(3)−2.300(3) Å, N−Ag−N 99.39-(12)−138.08(12)°) by three different μ_3-etz^- ligands. The silver-triazolate scaffold can be simplified as the common **dia** topology regarding the twisted $Ag_4(etz)_4$ circuits (linked by pyrazolate moieties of etz^- ligands) as tetrahedral nodes, and double Ag−N[4] bonds as linkers (Figure 3a). The straightforward 3-connected topology of **3** is more interesting. Although there are four crystallographically different 3-connected building blocks, they have identical point and vertex symbols of $8^2.10$ and $8.8_2.12$, respectively (Figure 3b).[17] This simple (uninodal) topology has only been theoretically predicted (sqc5603 deposited in EPINET)[18] rather than reported for crystal structures. As derived from the underlying topology, the silver triazolate scaffold of **3** contains intersecting channels. While the channels along the [1 0 1] direction are occupied by ethyl groups, those along the *c*-axis remain open (void = 14%, *d* = 3.4 Å), which are filled with disordered water molecules (Figure 3c). The trigonally coordinated Ag^+ ions are exposed on the pore surface. The related porous structures of **3** can be ascribed to the fact that sqc5603 (0.3828 Å^{-3}) has a lower topology density than **utp** (0.4218 Å^{-3}). It should be noted that sqc5603 and **utp** are relatively dense 3-connected nets, but their topology density is still lower than those of the very open zeolitic nets such as RHO and LTA, which should be ascribed to the fact that

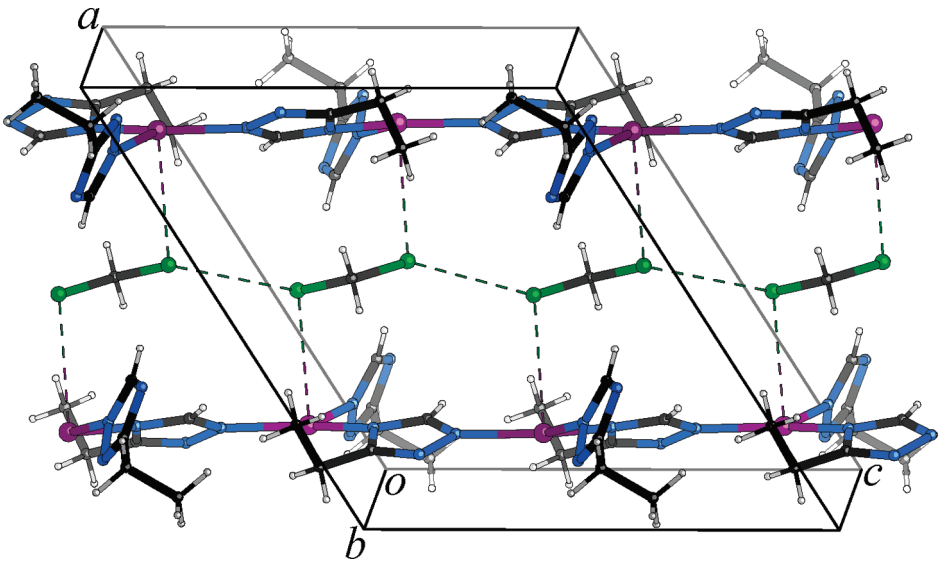

Figure 4. Perspective view of the structure of **3**·CH_2Cl_2 (host−guest and guest−guest contacts are shown in dashed lines).

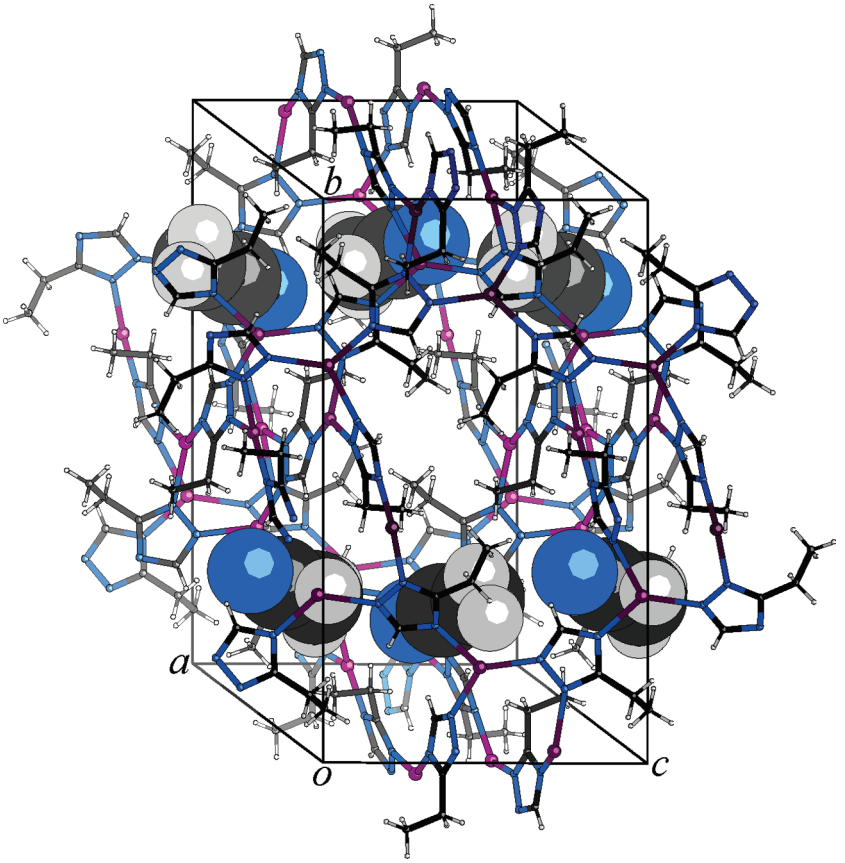

Figure 5. Perspective view of the structure of **3**·CH_3CN (CH_3CN molecules are highlighted in space filling mode).

low-connectivity topologies generally have low density (Table 2).[19] More importantly, the silver-triazolate scaffold in **3**·H_2O (V = 2764 Å^3) is not significantly contracted (−16%) from its most expanded configuration (V = 3285 Å^3 with edge length 3.4 Å). For comparison, **1** (V = 465 Å^3) and **2** (V = 558 Å^3) are contracted −38% and −24%, respectively, from the most expanded **utp** net (V = 745 Å^3 with edge length 3.4 Å). While compound **4** is isostructural with **3**, the presence of long propyl groups renders a virtually nonporous (void = 7%) structure, and no guest molecule is found (Figure S8).

Porous Property. According to TG analysis, **3**·H_2O can lose all guest molecules below 110 °C and decomposes above 250 °C (Figure S9). Single-crystal X-ray diffraction study of guest-free **3** confirms the removal of guest molecules and slight contraction (a −1.2%, b −0.8%, V −1.1%) of the host framework (Figure S10). However, the activated sample of **3** does not show N_2 adsorption at 77 K, which resembles some

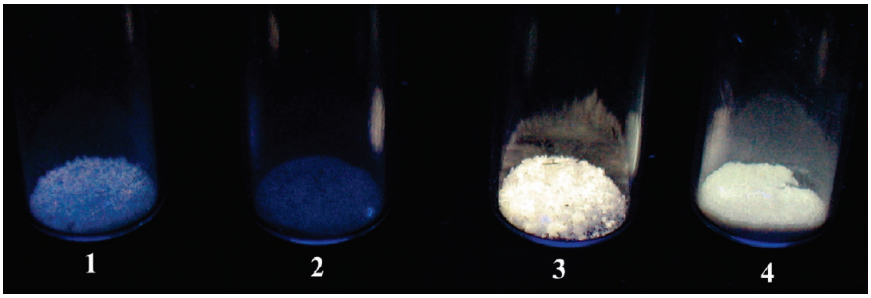

Figure 6. A photograph of **1**, **2**, **3**, and **4** under UV (365 nm) irradiation.

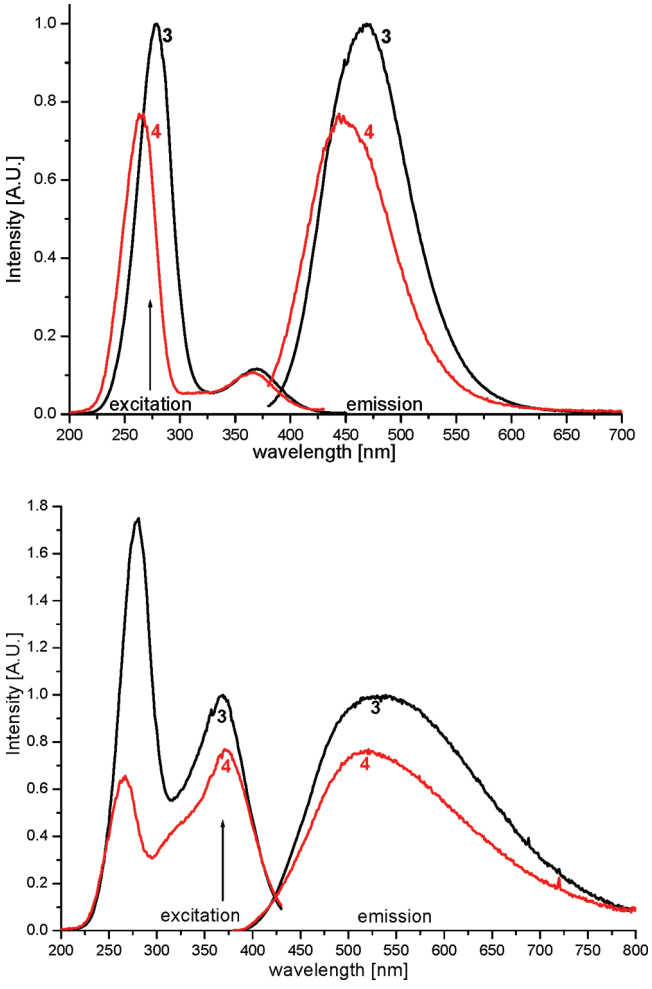

Figure 7. Blue (top) and near-white (bottom) photoluminescence spectra of **3** and **4**.

microporous materials with very small channels.[20] On the other hand, **3**·H_2O can readily undergo solvent exchange, and **3** can also adsorb solvent vapor, to give CH_2Cl_2 and CH_3CN included phases, whose structures were also determined by single-crystal X-ray diffraction.

3·CH_2Cl_2 is isomorphous to **3**·H_2O and **3**, containing two Ag^+ ions, two etz^- ligands, and half of a CH_2Cl_2 molecule in the asymmetric (Figure S11). The C atom of the C_2 symmetric CH_2Cl_2 molecule resides at the crystallographic 2-fold axis. Compared to the guest-free **3**, the unit cell volume of **3**·CH_2Cl_2 is expanded as a result of the insertion of guest molecules. However, the *a*-axis of **3**·CH_2Cl_2 is slightly contracted (−0.54%), indicating attractive interaction between CH_2Cl_2 and the host framework. Detailed analysis shows that the Cl atom of CH_2Cl_2 and the Ag^+ ion on the pore surface exhibit close contact (3.44 Å), which is slightly shorter than the sum of the van der Waals radii of Cl (1.75 Å) and Ag (1.72 Å). Inside the 1D channel, adjacent CH_2Cl_2 molecules also have relatively short Cl···Cl separations (3.55 Å) (Figure 4).

In contrast with other analogues, **3**·CH_3CN crystallizes in the space group of $P2_1/c$, with four Ag^+ ions, four etz^- ligands, and a complete CH_3CN molecule in the asymmetric unit (Figure S12). The symmetry lowering should arise from the presence of CH_3CN, which locates at but is not compatible with the 2-fold axis of the original space group $C2/c$. While CH_3CN molecules array in the head-to-tail fashion to form a polar supramolecular chain, these chains run in opposite directions in different channels and cancel their polarity (Figure 5). After inclusion of CH_3CN, the silver-triazolate scaffold also undergoes significant distortion, which can be judged by their very different β angles.

Luminescent Property. Under UV irradiation, the photoluminescence intensities of the **utp** (**1** and **2**) and sqc5603 (**3** and **4**) structures are distinctly different (Figure 6), indicating that the network topologies and/or framework distortions may have significant influence on the nonradiative decay processes. Interestingly, **3** and **4** both exhibit dual-mode photoluminescence, i.e., each compound has two distinct emission profiles depending on the excitation wavelengths. For instance, upon high-energy excitation (maximum at 280 nm), **3** emits blue light (maximum at 470 nm). While the excitation energy is lowered (maximum at 370 nm), the emission profile is also red-shifted (maximum at 530 nm) (Figure 7). More remarkably, this low-energy emission profile is very broad, and the emission color is close to the white light, which are of particular application importance but have been rarely observed for coordination complexes.[21] Because the excitation band also well matches the commercially used UV light-emitted diode (LED) chip, **3** may be potentially useful for white LED applications. The photoluminescence behavior of **4** is similar to that of **3**. Such dual-mode photoluminescence properties were previously observed for the silver salt of unsubstituted 1,2,4-triazolate[9b] and 4-cyanobenzoate.[21b] The high- and low-energy emissions have been assigned to the ligand-based $^3[\pi-\pi^*]$ (heavy atom effect from three Ag ions coordinated to the same triazolate) and ligand-to-metal charge transfer ^{1}[LMCT] excited states.[9b] By virtue of the porosity of **3**, its luminescent intensity can be also tuned by guest inclusion.[22] As shown in Figure 8, the quenching effects of different guests follow $H_2O \gg CH_3CN > CH_2Cl_2$, which is probably related to their X−H (X = O or C) vibration frequencies. High vibration energy will efficiently enhance nonradioactive transition probability and, on the contrary, contribute to low emission intensity.[23]

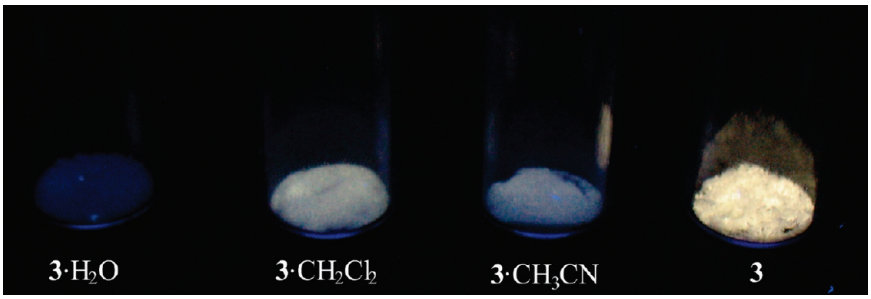

Figure 8. A photograph of **3**·H_2O, **3**·CH_2Cl, **3**·CH_3CN, and **3** under UV (365 nm) irradiation.

Conclusions

A series of silver(I) 3-alkyl-1,2,4-triazolates have been synthesized and characterized. The resultant new MAFs show novel uniform/uninodal 3-connected topologies, demonstrating that the size and position of substituent groups are crucial in controlling the framework topologies. Although the flexible triazolate frameworks tend to distort to form dense structures, it is still possible to obtain porous materials by using suitable substituent group and synthetic condition. The porous silver 3-ethyl-1,2,4-triazlate shows interesting framework flexibility and host−guest properties, which can be monitored by single-crystal X-ray diffraction and photoluminescence studies.

Acknowledgment. We thank Dr. Ng (University of Malaya) for single-crystal structure analysis. This work was supported by the "973 Program" (2007CB815302), NSFC (20821001 & 2100-1120), Chinese Ministry of Education (109125 & ROCS), and the Open Fund of the State Key Laboratory of Optoelectronic Materials and Technologies.

Supporting Information Available: Additional plots, TG analysis, and PXRD patterns (PDF), as well as X-ray data files (CIF). This material is available free of charge via the Internet at http://pubs.acs.org.

References

(1) (a) Janiak, C. *Dalton Trans*. **2003**, 2781. (b) Kitagawa, S.; Kitaura, R.; Noro, S. *Angew. Chem., Int. Ed.* **2004**, *43*, 2334. (c) Allendorf, M. D.; Bauer, C. A.; Bhakta, R. K.; Houk, R. J. T. *Chem. Soc. Rev*. **2009**, *38*, 1330. (d) Li, J.-R.; Kuppler, R. J.; Zhou, H.-C. *Chem. Soc. Rev*. **2009**, *38*, 1477. (e) Chen, B. L.; Xiang, S. C.; Qian, G. D. *Acc. Chem. Res*. **2010**, *43*, 1115.

(2) (a) Wells, A. F. *Three-Dimensional Nets and Polyhedra*; Wiley: New York, 1977. (b) Batten, S. R.; Robson, R. *Angew. Chem., Int. Ed*. **1998**, *37*, 1460. (c) Robson, R. *J. Chem. Soc., Dalton Trans*. **2000**, 3735. (d) Ockwig, N. W.; Delgado-Friedrichs, O.; O'Keeffe, M.; Yaghi, O. M. *Acc. Chem. Res*. **2005**, *38*, 176. (e) O'Keeffe, M.; Peskov, M. A.; Ramsden, S. J.; Yaghi, O. M. *Acc. Chem. Res*. **2008**, *41*, 1782. (f) Tranchemontagne, D. J.; Mendoza-Cortes, J. L.; O'Keeffe, M.; Yaghi, O. M. *Chem. Soc. Rev*. **2009**, *38*, 1257.

(3) (a) Masciocchi, N.; Galli, S.; Sironi, A. *Comments Inorg. Chem*. **2005**, *26*, 1. (b) Zhang, J.-P.; Chen, X.-M. *Chem. Commun*. **2006**, 1689.

(4) (a) Tian, Y. Q.; Cai, C. X.; Ji, Y.; You, X. Z.; Peng, S. M.; Lee, G. H. *Angew. Chem., Int. Ed.* **2002**, *41*, 1384. (b) Huang, X.-C.; Zhang, J.-P.; Chen, X.-M. *Chin. Sci. Bull*. **2003**, *48*, 1531. (c) Tian, Y. Q.; Yao, S. Y.; Gu, D.; Cui, K. H.; Guo, D. W.; Zhang, G.; Chen, Z. X.; Zhao, D. Y. *Chem.—Eur. J*. **2010**, *16*, 1137. (d) Phan, A.; Doonan, C. J.; Uribe-Romo, F. J.; Knobler, C. B.; O'Keeffe, M.; Yaghi, O. M. *Acc. Chem. Res*. **2010**, *43*, 58.

(5) (a) Abdou, H. E.; Mohamed, A. A.; Fackler, J. P.; Burini, A.; Galassi, R.; Lopez-de-Luzuriaga, J. M.; Olmos, M. E. *Coord. Chem. Rev*. **2009**, *253*, 1661. (b) Miras, H. N.; Chakraborty, I.; Raptis, R. G. *Chem. Commun*. **2010**, *46*, 2569.

(6) (a) Zhang, J.-P.; Horike, S.; Kitagawa, S. *Angew. Chem., Int. Ed*. **2007**, *46*, 889. (b) Zhang, J. P.; Kitagawa, S. *J. Am. Chem. Soc*. **2008**, *130*, 907.

(7) (a) Choi, H. J.; Dinca, M.; Long, J. R. *J. Am. Chem. Soc*. **2008**, *130*, 7848. (b) Tonigold, M.; Lu, Y.; Bredenkotter, B.; Rieger, B.; Bahnmuller, S.; Hitzbleck, J.; Langstein, G.; Volkmer, D. *Angew. Chem., Int. Ed*. **2009**, *48*, 7546. (c) Masciocchi, N.; Galli, S.; Colombo, V.; Maspero, A.; Palmisano, G.; Seyyedi, B.; Lamberti, C.; Bordiga, S. *J. Am. Chem. Soc*. **2010**, *132*, 7902.

(8) (a) Su, C. Y.; Goforth, A. M.; Smith, M. D.; Pellechia, P. J.; zur Loye, H. C. *J. Am. Chem. Soc*. **2004**, *126*, 3576. (b) Zhang, J. P.; Lin, Y. Y.; Zhang, W. X.; Chen, X. M. *J. Am. Chem. Soc*. **2005**, *127*, 14162. (c) Chen, S. P.; Sun, S.; Gao, S. L. *J. Solid State Chem*. **2008**, *181*, 3308. (d) Zhu, A.-X.; Lin, J.-B.; Zhang, J.-P.; Chen, X.-M. *Inorg. Chem*. **2009**, *48*, 3882. (e) Yang, G.; Raptis, R. G. *Chem. Commun*. **2004**, 2058. (f) Huang, X. H.; Sheng, T. L.; Xiang, S. C.; Fu, R. B.; Hu, S. M.; Li, Y. M.; Wu, X. T. *Inorg. Chem*. **2007**, *46*, 497. (g) Ouellette, W.; Yu, M. H.; O'Connor, C. J.; Hagrman, D.; Zubieta, J. *Angew. Chem., Int. Ed*. **2006**, *45*, 3497. (h) Ouellette, W.; Prosvirin, A. V.; Chieffo, V.; Dunbar, K. R.; Hudson, B.; Zubieta, J. *Inorg. Chem*. **2006**, *45*, 9346. (i) Ouellette, W.; Galan-Mascaros, J. R.; Dunbar, K. R.; Zubieta, J. *Inorg. Chem*. **2006**, *45*, 1909. (j) Ouellette, W.; Hudson, B. S.; Zubieta, J. *Inorg. Chem*. **2007**, *46*, 4887. (k) Ouelleffe, W.; Prosvirin, A. V.; Valeich, J.; Dunbar, K. R.; Zubieta, J. *Inorg. Chem*. **2007**, *46*, 9067. (l) Zhang, R. B.; Zhang, J.; Li, Z. J.; Cheng, J. K.; Qin, Y. Y.; Yao, Y. G. *Cryst. Growth Des*. **2008**, *8*, 3735. (m) Kuang, X. F.; Wu, X. Y.; Yu, R. M.; Donahue, J. P.; Huang, J. S.; Lu, C. Z. *Nat. Chem*. **2010**, *2*, 461. (n) Park, H.; Britten, J. F.; Mueller, U.; Lee, J.; Li, J.; Parise, J. B. *Chem. Mater*. **2007**, *19*, 1302.

(9) (a) Zhang, J.-P.; Zheng, S.-L.; Huang, X.-C.; Chen, X.-M. *Angew. Chem., Int. Ed*. **2004**, *43*, 206. (b) Zhang, J. P.; Lin, Y. Y.; Huang, X. C.; Chen, X. M. *J. Am. Chem. Soc*. **2005**, *127*, 5495.

(10) (a) Zhang, J.-P.; Chen, X.-M. *J. Am. Chem. Soc*. **2008**, *130*, 6010. (b) Yang, C.; Wang, X.; Omary, M. A. *J. Am. Chem. Soc*. **2007**, *129*, 15454.

(11) (a) Huang, X. C.; Zhang, J. P.; Chen, X. M. *J. Am. Chem. Soc*. **2004**, *126*, 13218. (b) Huang, X.-C.; Lin, Y.-Y.; Zhang, J.-P.; Chen, X.-M. *Angew. Chem., Int. Ed*. **2006**, *45*, 1557.

(12) Yang, G.; Zhang, P. P.; Liu, L. L.; Kou, J. F.; Hou, H. W.; Fan, Y. T. *CrystEngComm* **2009**, *11*, 663.

(13) Jones, R. G.; Ainsworth, C. *J. Am. Chem. Soc*. **1955**, *77*, 1538.

(14) Sheldrick, G. M. *SHELXTL 6.12*; Bruker Analytical Instrumentation: Madison, WI, 2000.

(15) Zhang, J.-P.; Lin, Y.-Y.; Huang, X.-C.; Chen, X.-M. *Dalton Trans*. **2005**, 3681.

(16) (a) Zhang, J.; Chen, Y. B.; Chen, S. M.; Li, Z. J.; Cheng, J. K.; Yao, Y. G. *Inorg. Chem*. **2006**, *45*, 3161. (b) Li, J. R.; Yu, Q.; Tao, Y.; Bu, X. H.; Ribas, J.; Batten, S. R. *Chem. Commun*. **2007**, 2290.

(17) Blatov, V. A.; O'Keeffe, M.; Proserpio, D. M. *CrystEngComm* **2010**, *12*, 44.

(18) EPINET, see http://epinet.anu.edu.au/.

(19) RCSR, see http://rcsr.anu.edu.au.

(20) Dybtsev, D. N.; Chun, H.; Yoon, S. H.; Kim, D.; Kim, K. *J. Am. Chem. Soc*. **2004**, *126*, 32.

(21) (a) Ki, W.; Li, J. *J. Am. Chem. Soc*. **2008**, *130*, 8114. (b) Wang, M. S.; Guo, S. P.; Li, Y.; Cai, L. Z.; Zou, J. P.; Xu, G.; Zhou, W. W.; Zheng, F. K.; Guo, G. C. *J. Am. Chem. Soc*. **2009**, *131*, 13572.

(22) (a) Huang, Y. Q.; Ding, B.; Song, H. B.; Zhao, B.; Ren, P.; Cheng, P.; Wang, H. G.; Liao, D. Z.; Yan, S. P. *Chem. Commun*. **2006**, 4906. (b) Chen, B. L.; Wang, L. B.; Xiao, Y. Q.; Fronczek, F. R.; Xue, M.; Cui, Y. J.; Qian, G. D. *Angew. Chem., Int. Ed*. **2009**, *48*, 500. (c) Chen, B. L.; Wang, L. B.; Zapata, F.; Qian, G. D.; Lobkovsky, E. B. *J. Am. Chem. Soc*. **2008**, *130*, 6718.

(23) (a) Zaitoun, M. A.; Goken, D. M.; Bailey, L. S.; Kim, T.; Lin, C. T. *J. Phys. Chem. B* **2000**, *104*, 189. (b) Lis, S. *J. Alloys Compd*. **2002**, *341*, 45. (c) Bischof, C.; Wahsner, J.; Scholten, J.; Trosien, S.; Seitz, M. *J. Am. Chem. Soc*. **2010**, *132*, 14334.